ARTICLE

Homozygous mutations in *C14orf39/SIX6OS1* cause non-obstructive azoospermia and premature ovarian insufficiency in humans

Suixing Fan,[1,4] Yuying Jiao,[1,4] Ranjha Khan,[1,4] Xiaohua Jiang,[1,4] Abdul Rafay Javed,[1] Asim Ali,[1] Huan Zhang,[1] Jianteng Zhou,[1] Muhammad Naeem,[2] Ghulam Murtaza,[1] Yang Li,[1] Gang Yang,[1] Qumar Zaman,[1] Muhammad Zubair,[1] Haiyang Guan,[1] Xingxia Zhang,[1] Hui Ma,[1] Hanwei Jiang,[1] Haider Ali,[1] Sobia Dil,[1] Wasim Shah,[1] Niaz Ahmad,[3] Yuanwei Zhang,[1,*] and Qinghua Shi[1,*]

Summary

Human infertility is a multifactorial disease that affects 8%–12% of reproductive-aged couples worldwide. However, the genetic causes of human infertility are still poorly understood. Synaptonemal complex (SC) is a conserved tripartite structure that holds homologous chromosomes together and plays an indispensable role in the meiotic progression. Here, we identified three homozygous mutations in the SC coding gene *C14orf39/SIX6OS1* in infertile individuals from different ethnic populations by whole-exome sequencing (WES). These mutations include a frameshift mutation (c.204_205del [p.His68Glnfs*2]) from a consanguineous Pakistani family with two males suffering from non-obstructive azoospermia (NOA) and one female diagnosed with premature ovarian insufficiency (POI) as well as a nonsense mutation (c.958G>T [p.Glu320*]) and a splicing mutation (c.1180−3C>G) in two unrelated Chinese men (individual P3907 and individual P6032, respectively) with meiotic arrest. Mutations in *C14orf39* resulted in truncated proteins that retained SYCE1 binding but exhibited impaired polycomplex formation between C14ORF39 and SYCE1. Further cytological analyses of meiosis in germ cells revealed that the affected familial males with the *C14orf39* frameshift mutation displayed complete asynapsis between homologous chromosomes, while the affected Chinese men carrying the nonsense or splicing mutation showed incomplete synapsis. The phenotypes of NOA and POI in affected individuals were well recapitulated by *Six6os1* mutant mice carrying an analogous mutation. Collectively, our findings in humans and mice highlight the conserved role of C14ORF39/SIX6OS1 in SC assembly and indicate that the homozygous mutations in *C14orf39/SIX6OS1* described here are responsible for infertility of these affected individuals, thus expanding our understanding of the genetic basis of human infertility.

Introduction

Human infertility, defined as the failure to achieve a clinical pregnancy after 12 months or more of regular unprotected sexual intercourse,[1] is estimated to affect 8%–12% of reproductive-aged couples worldwide.[2] The etiology of human infertility is multifactorial, and genetic factors have been proposed to be involved in most cases.[3] Although aberrations in the number and structure of chromosomes can explain a proportion of the affected individuals, the etiology and pathology for the large remaining number of infertile individuals, for whom single-gene variants could be the underlying causes, are still unclear.[4] To date, several genes, such as *STAG3* (MIM: 608489), *BRCA2* (MIM: 600185), *TEX11* (MIM:300311), *HFM1* (MIM: 615684), and *SHOC1* (MIM: 618038), have been associated with non-obstructive azoospermia (NOA) or premature ovarian insufficiency (POI).[5–11] However, compared with the known genetic defects in more than 400 genes affecting mouse fertility,[12] little is known about the genetic basis of human infertility.

Synaptonemal complex (SC), formed between paired homologous chromosomes during the prophase of meiosis I, is a conserved zipper-like structure that facilitates interhomolog crossover formation and successful production of gametes. The fully formed SC is composed of two parallel lateral elements (LEs) and a single central element (CE), which are bridged by numerous transverse filaments (TFs). So far, eight SC components have been identified in mammals, including two LE proteins, SYCP3 and SYCP2; one TF protein, SYCP1; and five CE proteins, SYCE1, SYCE2, SYCE3, TEX12, and SIX6OS1.[13] Genetic disruption in any of them invariably causes mouse infertility,[14–19] except for *Sycp3* and *Sycp2* female mutant mice, which are subfertile.[20,21] However, only mutations in *SYCP3* (MIM: 604759), *SYCE1* (MIM: 611486), and *SYCP2* (MIM: 604105) have been associated with human infertility,[22–25] although the pathogenicity of these mutations was determined by *in silico*

[1]Division of Reproduction and Genetics, First Affiliated Hospital of USTC, Hefei National Laboratory for Physical Sciences at Microscale, the CAS Key Laboratory of Innate Immunity and Chronic Disease, School of Basic Medical Sciences, Division of Life Sciences and Medicine, CAS Center for Excellence in Molecular Cell Science, Collaborative Innovation Center of Genetics and Development, University of Science and Technology of China, Hefei 230027, China; [2]Medical Genetics Research Laboratory, Department of Biotechnology, Quaid-i-Azam University, Islamabad 45320, Pakistan; [3]Shahbaz Sharif District Hospital, Multan 60800, Pakistan
[4]These authors contributed equally
*Correspondence: zyuanwei@ustc.edu.cn (Y.Z.), qshi@ustc.edu.cn (Q.S.)
https://doi.org/10.1016/j.ajhg.2021.01.010.

analysis or deduced from studies of knockout mice rather than by functional identification using animal models with the same mutation. Recently, humanized mutant mice were generated to evaluate the pathogenicity of the *SYCE1* nonsense mutation (c.721C>T [p.Gln241*]) discovered in POI-affected individuals, which did not result in a truncated protein but induced nonsense-mediated mRNA degradation.[25]

C14orf39 (MIM: 617307) is the ortholog of murine *Six6os1*, which encodes a CE component of the SC and specifically interacts with SYCE1 via its α-helical domain.[19] Knockout of *Six6os1* in mice resulted in chromosomal asynapsis and meiotic arrest, which eventually led to azoospermia and ovarian failure.[19] A heterozygous missense variant in *C14orf39* (c.1570C>T [p.Leu524Phe]) was associated with higher recombination rates in human females, but not in males, in the Icelandic population.[26] In contrast, another genome-wide association study conducted in the US population showed a strong association between *C14orf39* and the recombination rate in males.[27] Although these findings could be explained by ethnic differences, the relation between *C14orf39* mutations and human fertility remains uncertain.

Here, we identified three pathogenic homozygous variants in *C14orf39/SIX6OS1* (GenBank: NM_174978.3) from a consanguineous Pakistani infertile family with two males suffering from NOA and one female diagnosed with POI and two Chinese NOA-affected individuals. Functional analyses showed that the affected males displayed severe synaptic defects and meiotic arrest and, consequently, azoospermia. The pathogenicity of these mutations is validated by the *Six6os1* mutant mouse model, which recapitulated the phenotypes of the NOA- and POI-affected individuals.

Material and methods

Clinical samples

Fifty consanguineous Pakistani families with at least two infertile siblings in each and 60 infertile Chinese men with meiotic arrest were collected. After we obtained informed consent, the individuals donated blood samples and testicular tissues for scientific research. Routine semen analyses were performed at least twice according to the WHO guidelines.[28] The reproductive hormones in the serum of individuals were determined in the local laboratory. The karyotype analyses of all individuals and the ultrasound examination of the affected female's reproductive system were performed in the local hospitals. This study was approved by the institutional ethics committee of the University of Science and Technology of China (USTC) with the approval number 2019-KY-168.

WES and variant filtration

WES was performed as we previously described.[29] Variants of the Pakistani family were filtered according to the following criteria: (1) variants that conform to the autosomal recessive inheritance were included; (2) variants located in the linkage regions with the logarithm of the odds scores >0.58 were included;[30] (3) variants with minor allele frequencies >0.05 in any of the public databases, including 1000 Genomes project, ESP6500, or gnomAD database, and variants that were homozygous in our in-house WES database generated from 578 fertile men (41 Pakistani, 254 Chinese, and 283 European) were excluded; (4) variants potentially affecting protein sequence (nonsense, missense, splice-site variants, and coding indels) were included; (5) variants within genes not expressed in the testis were excluded; (6) variants predicted to be deleterious by more than half of the software (provided by ANNOVAR) covering them were included;[31] and (7) variants within genes dispensable for spermatogenesis in mice on the basis of SpermatogenesisOnline1.0 or literature search were excluded.[32] The remaining variants were subsequently verified by Sanger sequencing in all the available family members. Primer sequences are shown in Table S2, and the flow chart of the variant filtering process is described in Figure S1.

Spermatocyte nuclear surface spreading and immunofluorescence staining

The surface spreads of spermatocytes were prepared according to previously described protocols.[33,34] For immunofluorescence, slides were blocked with 3% nonfat milk in phosphate-buffered saline (PBS) for 30 min and then incubated with primary antibodies overnight at 37°C in a humidified chamber. After three washes in PBS containing 0.05% Triton X-100 (PBST), secondary antibodies were applied for 1 h at 37°C. Subsequently, the slides were washed three times in PBST and mounted with the Vectashield Medium (Vector Laboratories, H-1000). Images were captured with an Olympus BX61 microscope with a CCD camera (QImaging, QICAM Fast 1394) and processed with Image-Pro Plus software (Media Cybernetic). The antibodies are listed in Table S1.

Quantitative polymerase chain reaction

Total RNAs were extracted with RNAiso Plus reagents (TaKaRa, 9109), and the cDNAs were synthesized with the PrimeScript RT reagent kit (TaKaRa, RR047A) according to the manufacturer's protocol. The quantitative polymerase chain reaction (qPCR) was performed with TransStart Top Green qPCR SuperMix (TransGen Biotech, AQ132) and a StepOne Real-Time PCR System (Applied Biosystems). We calculated relative mRNA levels by normalizing to *ACTB* (MIM: 102630). The relative mRNA levels in the control were regarded as 1, and the fold changes in the affected individuals were compared to this. Primer sequences are listed in Table S2.

Yeast two-hybrid assay

C14orf39 was cloned from human testis cDNA with the PrimeStar HS DNA Polymerase (TaKaRa, R010A) and then inserted into the pGADT7 vector and transformed into Y187 stain as prey. Mouse *Syce1* was cloned from mouse testis cDNA, inserted into the pGBKT7 vector, and transformed into Y2HGold strain as bait. The mutagenesis was accomplished by overlap PCR. The construction of the plasmids was achieved by homologous recombination with the Exnase enzyme (Vazyme, C113). Yeast transformation was conducted according to the manual (PT1172-1) from Clontech Laboratories, and two-hybrid assays were performed as we previously described.[33] We plated the mating products on SD/−Trp/−Leu (−LW) and SD/−Trp/−Leu/−His/−Ade (−LWHA) plates for 3–5 days to test the interactions. The pGBKT7 and pGADT7 vectors were used as negative control.

Polycomplex formation

Wild-type and mutated *C14orf39* coding sequences were fused to the C terminus of EGFP, and the coding sequence of *SYCE1* (GenBank: NM_001143765.1) was fused to the C terminus of mCherry. COS-7 cells (SCSP-508) were kindly provided by Stem Cell Bank (Chinese Academy of Sciences) and cultured in 24-well plates with a coverslip at the bottom and transfected with the vectors with Lipofectamine 3000 according to the manufacturer's instructions. After 36 h of transfection, the cells were fixed in 4% polyformaldehyde for 10 min and the nuclei were stained with Hoechst 33342 (Invitrogen, H21492). After three washes in PBS, the coverslips were mounted on slides with Vectashield Medium. The images were captured with a Nikon Eclipse Ti2 inverted microscope with a C2 plus laser scanning confocal head under the control of NIS elements imaging software version 5.01.

Histological analysis

Testicular tissues were fixed in Bouin's solution overnight and then embedded into the paraffin and sectioned at 5 μm thickness. The tissue slides were deparaffinized by xylene and rehydrated with gradient ethanol and then sequentially stained with hematoxylin and eosin. After dehydration and transparency, the tissue sections were sealed with neutral resin. Ovaries were fixed with 4% formaldehyde solution and only stained with hematoxylin. The images were captured via a Nikon ECLIPSE 80i microscope with a DR-Ri1 camera and processed with NIS-elements BR software. Immunofluorescence staining on the testicular sections was conducted as we previously described.[35] The antibodies are listed in Table S1.

Generation of *Six6os1* mutant mice

Six6os1 (GenBank: NM_029444.2) mutant mice carrying mutation analogous to the affected individuals was generated via CRISPR/Cas9 technology as we described previously.[33] The sgRNA sequence and primers used for genotyping are listed in Table S2. The mice were maintained under specific-pathogen-free conditions in the laboratory animal center of USTC. All experiments involving animals were approved by the institutional animal ethics committee of USTC.

Statistical analysis

Statistical significance was assessed with an unpaired, two-tailed Student's t test or Welch's t test. All p values and statistical tests were specified in the text and figure legends. A p value of <0.05 was considered statistically significant.

Results

Identification of *C14orf39* pathogenic variants

To reveal the genetic causes of human infertility, we have collected 50 consanguineous Pakistani families with at least two infertile siblings in each and 60 Chinese men with meiotic arrest. Among them, *C14orf39* mutations were identified from one consanguineous Pakistani family and two Chinese men (Figure 1A). For the family PK-INF-543, we performed WES analyses of the two affected individuals with NOA (IV-2 and IV-3), the two fertile brothers (IV-1 and IV-4), and their mother (III-2) (Figure 1A). More than 400,000 variants per individual were detected from the WES data that covered at least 99% of the targeted sequence at 90× or greater depth. Considering that the individuals were born to a consanguineous marriage, variants following autosomal recessive inheritance were prioritized. These variants were filtered with a series of criteria, and two candidate pathogenic variants, a 1-bp insertion in *DHRS4L2* (c.629_630insA [p.His211Alafs*69] [MIM: 615196] [GenBank: NM_198083.4]) and a 2-bp deletion in *C14orf39* (c.204_205del [GenBank: NM_174978.3]) were identified (Figure S1). To determine the transmission patterns of these variants in this family, we performed targeted Sanger sequencing in all available family members. The *DHRS4L2* variant was ruled out because of its heterozygosity in the diseased sister, IV-5 (Figure S2). Only the mutation in *C14orf39* conformed to Mendelian segregation in all family members. This frameshift variant was confirmed at the mRNA level in testicular tissues of individual IV-3 (Figures 1A and S3). Besides, this *C14orf39* variant (c.204_205del [p.His68Glnfs*2]) is absent in the 1000 Genomes Project database and has low frequencies in the ESP6500 and gnomAD databases (Table S3). Given that this homozygous mutation is expected to cause 520 amino acid deletions in the full-length C14ORF39 protein consisting of 587 amino acids, and the meiotic arrest phenotype of *Six6os1* knockout mice, we think that the mutation in *C14orf39* (c.204_205del [p.His68Glnfs*2]) is the most likely pathogenic variant in this family.

We also identified two other *C14orf39* homozygous mutations as the only candidate pathogenic variants in two Chinese men with meiotic arrest. Individual P3907 had a nonsense mutation (c.958G>T [p.Glu320*]), and individual P6032 carried a splicing mutation (c.1180−3C>G). Both variants were validated by Sanger sequencing and have not been reported in any public databases (Figure 1A and Table S3). Therefore, three pathogenic variants in *C14orf39* were identified in infertile individuals of different ethnic groups (Figure 1B), implying that C14ORF39 provides a genetic contribution to human fecundity.

Clinical characteristics of the affected individuals

On the basis of the WHO guidelines, at least two semen analyses were conducted in affected individuals IV-2 and IV-3 and showed that they had normal semen volume but no sperm (Table 1). To examine the spermatogenesis of individuals carrying homozygous *C14orf39* mutations, we obtained testicular biopsies from three affected men (IV-3, P3097, and P6032) and a control man. H&E staining on the testicular sections revealed that many spermatogenic cells, including spermatogonia, spermatocytes, and spermatozoa, were observed in the seminiferous tubules of the control, whereas in the affected individuals, spermatogonia and spermatocytes were found, but post-meiotic cells were absent in all of their available seminiferous tubules (Figure 1C). These results indicated that the affected males suffered from non-obstructive azoospermia and their spermatogenesis was arrested at the spermatocyte stage. Notably, the unmarried sister (IV-5, 30 years

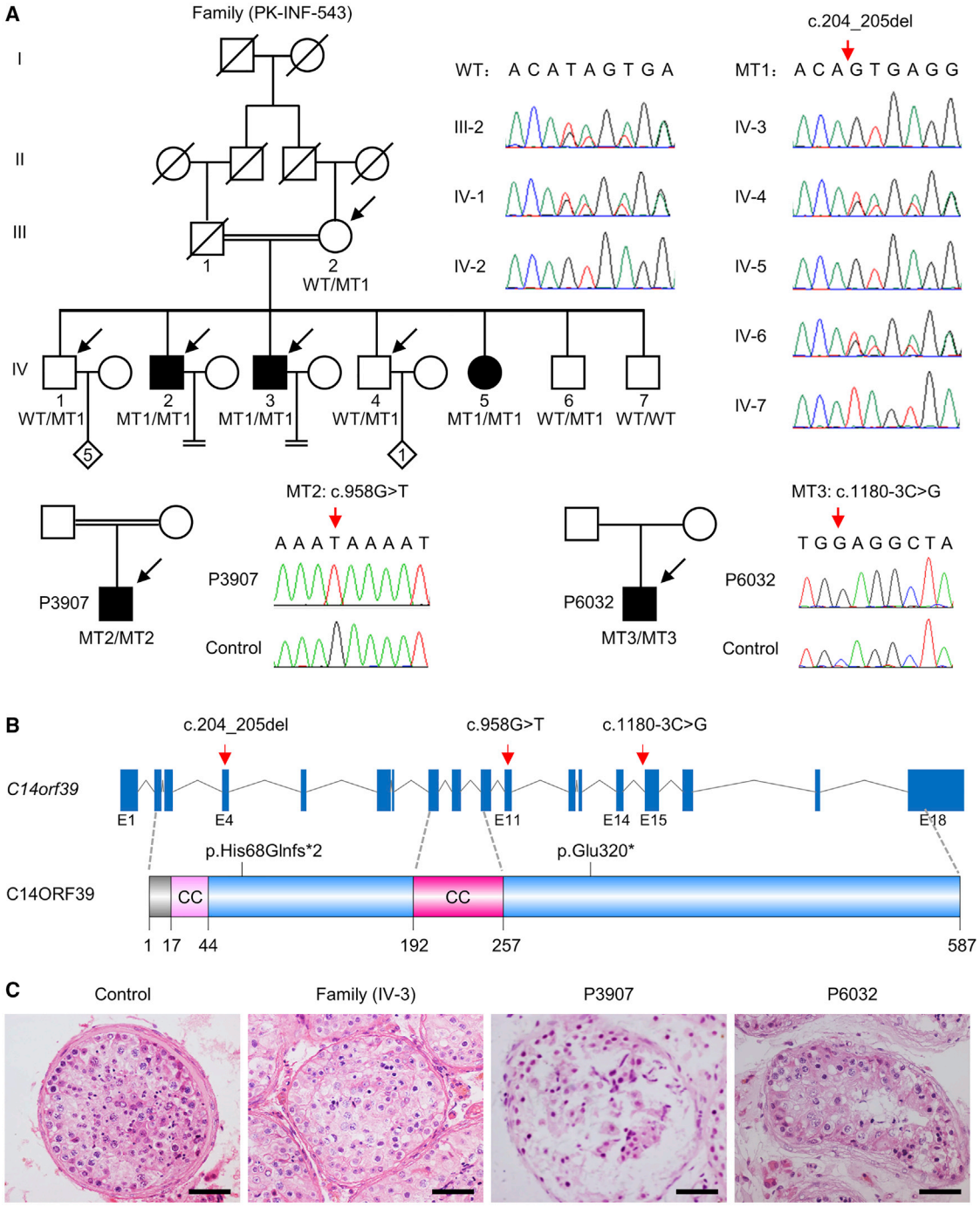

Figure 1. Identification of homozygous variants in *C14orf39* from NOA- and POI-affected individuals

(A) The pedigrees of the families. Double horizontal lines represent the consanguineous unions. Squares and circles denote male and female members, respectively. The number in the diamond indicates the number of offspring whose gender is unknown. Solid symbols indicate the affected members, and open symbols denote unaffected members. Slashes represent deceased members, and the equal sign indicates infertility. Members indicated by arrows were selected for whole-exome sequencing. Sanger sequencing chromatograms of *C14orf39* are shown on the right side. The red arrows indicate the corresponding mutations.

(B) Schematic map of the mutation positions in *C14orf39* at the genomic and protein levels. The gene composition is based on the Ensembl database (GRCh38, transcript ID: ENST00000321731.8). The blue solid squares represent exons, and the lines represent introns. Two putative coiled-coil (CC) domains of C14ORF39 were predicted by the web-based COILS program.

(C) Histological analyses of human testicular tissues by H&E staining. Scale bars indicate 50 μm.

old) in the family PK-INF-543 was considered as an individual with POI,[36] characterized by irregular menstrual cycles, amenorrhea at the age of 24, high levels of follicle-stimulating hormone and luteinizing hormone, and low levels of anti-Müllerian hormone (Table 1 and Supplemental notes).

Table 1. Clinical characteristics of the family members

	Ref values	IV-1	IV-2	IV-3	IV-4	IV-5	IV-6	IV-7	III-1
Age (years)[a]	–	43	40	37	33	30	28	24	58
Gender	–	M	M	M	M	F	M	M	F
Height/weight (cm/kg)	–	176/74	178/69	170/71	172/66	164/54	174/65	169/62	166/60
Karyotype	–	46,XY	46,XY	46,XY	46,XY	46,XX	46,XY	46,XY	46,XX
Diagnosis of disease	–	–	NOA	NOA	–	POI	–	–	–
Semen analysis[b]									
Semen volume (mL)	>1.5	3.0	2.5 ± 0.87	2.0 ± 0.41	–	–	–	–	–
Sperm count (millions/mL)	>15	42	0	0	–	–	–	–	–
Hormone analysis[c]									
Testosterone (ng/dL)	249–836	–	436.5	426.1	–	–	–	–	–
FSH (mIU/mL)	M: 1.4–15.4 F: 1.4–9.9	–	7.41	6.79	–	49.06	–	–	–
LH (mIU/mL)	M: 1.2–7.8 F: 1.7–15	–	4.83	3.95	–	47.69	–	–	–
Progesterone (ng/mL)	M: 0.2–1.22 F: 0.1–1.40	–	0.37	0.24	–	0.21	–	–	–
Prolactin (ng/mL)	M: 3–14.7	–	6.42	9.86	–	–	–	–	–
AMH (ng/mL)	F: 0.9–9.5	–	–	–	–	0.021	–	–	–
Physical examination[d]									
Ovaries (mL)	>3.5	–	–	–	–	L: 1 mL; R: invisible	–	–	–
Uterus (cm*cm)	>9*8	–	–	–	–	5.5*2.1	–	–	–

Ref, reference; NOA, non-obstructive azoospermia; POI, premature ovarian insufficiency; M, male; F, female; FSH, follicle-stimulating hormone; LH, luteinizing hormone; AMH, anti-Müllerian hormone; L, left; R, right.
[a]Ages at the manuscript submission.
[b]Reference values were published by WHO in 2010.
[c]Reference values were suggested by the local clinical laboratory.
[d]Physical examination was performed by a consultant gynecologist.

Effects of the identified mutations on *C14orf39* expression

Considering that both the *C14orf39* frameshift mutation (c.204_205del) and nonsense mutation (c.958G>T) introduce a premature stop codon, these mutations may result in mRNA degradation or truncated proteins. To test these possibilities, we first performed qPCR and reverse-transcription PCR (RT-PCR) to evaluate the relative transcriptional expression of *C14orf39*. The mRNA levels of *C14orf39* in the testis of individual IV-3, carrying the homozygous frameshift mutation, were 56.4% of that in the control ($p = 0.0527$; Welch's t test; Figure 2A), and individual P3907, harboring the homozygous nonsense mutation, showed comparable expression to the control group (Figure 2B). To clarify whether these mutations result in truncated proteins, we expressed wild-type and mutated C14ORF39 with an N-terminal EGFP fusion in COS-7 cells, followed by immunoblot examination. The mutant proteins were observed at the expected sizes (Figure 2C), indicating that these *C14orf39* mutations led to the production of truncated proteins.

Synaptic defects and meiotic arrest were observed in individuals with homozygous *C14orf39* mutations

To test whether these mutations in *C14orf39* affected the assembly of SCs *in vivo*, we obtained testicular biopsies from affected males and prepared spermatocyte spreads for subsequent immunofluorescence staining. For individual IV-3 from the family PK-INF-543, we first stained the spermatocyte spreads for SYCP3 and SYCP1 to assess chromosome synapsis (Figure 3A). In control cells, SYCP1 signals first appeared as short stretches between the paired chromosomes at zygotene and extended to the full length of the chromosomal axes at pachytene. In spermatocytes of individual IV-3, however, the SYCP1 signal was undetectable on the chromosomal axes, even in the most advanced spermatocytes, when fully assembled lateral elements were extensively co-aligned in some regions. Consistent with this finding, the SYCE1 signals were also absent from the chromosomal axes of spermatocytes in individual IV-3 (Figure 3B). These results indicated that the *C14orf39* frameshift mutation (c.204_205del [p.His68Glnfs*2]) caused complete asynapsis of homologous chromosomes.

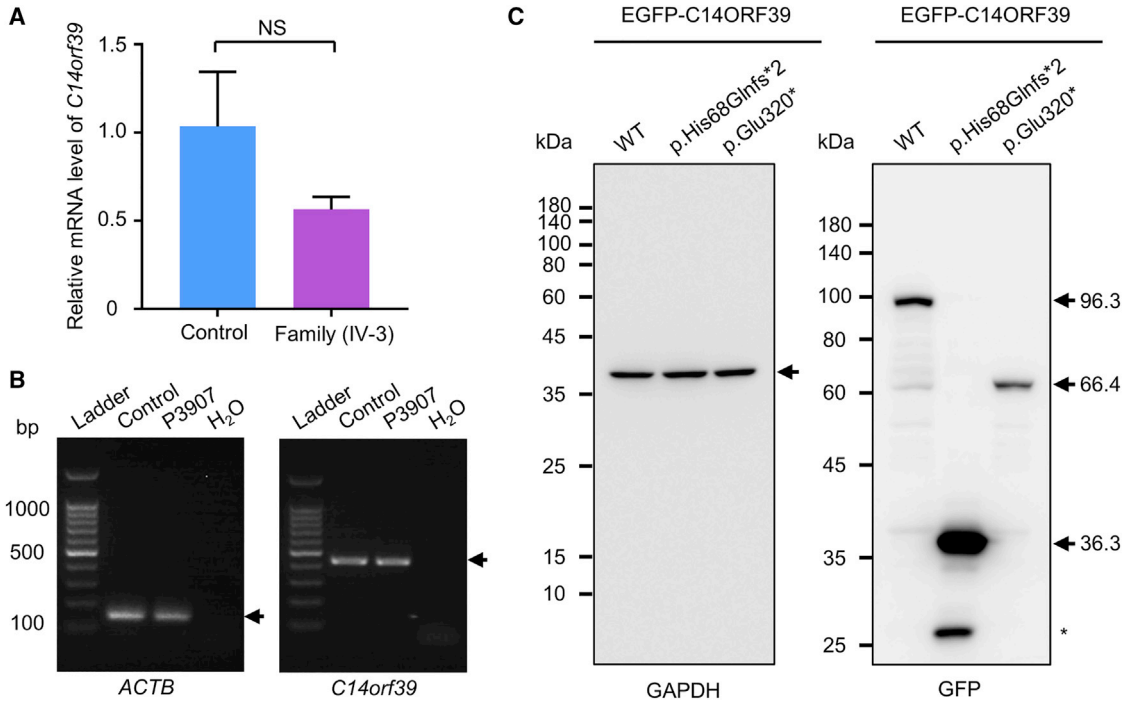

Figure 2. The effects of *C14orf39* mutations on gene expression

(A) Quantitative PCR analyses of the relative *C14orf39* expression in the testes from the control and individual IV-3. Data are from four repeated experiments and represent means ± SD. Statistical significance was determined using Welch's t test. NS, not significant. *ACTB* was used as an internal control.

(B) RT-PCR analysis of blood samples from a man with obstructive azoospermia and individual P3907 carrying the *C14orf39* nonsense mutation (c. 958G>T [p.Glu320*]). *ACTB* served as a loading control. Arrows indicate targeted bands.

(C) Heterologous expression of C14ORF39 in COS-7 cells. N-terminal EGFP-fused wild-type (WT) and two mutated *C14orf39* (c.204_205del [p.His68Glnfs*2] and c.985G>T [p.Glu320*]) plasmids were transfected into COS-7 cells. After 36 h of transfection, whole-cell lysates were prepared and separated by SDS-PAGE. C14ORF39 was detected by GFP antibody and GAPDH served as a loading control. Arrows indicate the targeted proteins, and the asterisk indicates non-specific band.

Because severe synaptic defects always cause meiotic arrest in mammals,[37] we thus examined the progression of meiotic prophase I by immunostaining the spermatocytes for SYCP3 and γH2AX, a marker of DNA breaks. Consistent with our previous report,[38] for the control, we observed that 33.6% of spermatocytes were at leptotene and zygotene, characterized by small patches and bright focal domains of γH2AX signals, respectively, and 66.4% of spermatocytes at pachytene showed a typical sex body with intense γH2AX signals around the X and Y chromosomes. For individual IV-3, after analyzing 644 spermatocytes, we found that the leptotene and zygotene nuclei were similar to that of the control, however, the most advanced spermatocytes displayed shorter and thicker LEs but persistent γH2AX signals on autosomes and failed to form sex body (Figure 3C). These results indicated that meiosis was arrested at the pachytene-like stage in affected individual IV-3.

For individual P3907, we performed immunofluorescence staining on testicular sections by using antibodies recognizing the middle segment (C14ORF39-M) or C terminus of C14ORF39 (C14ORF39-C) (Figure S4). To examine the progression of meiotic prophase I, we used the γH2AX antibody concurrently. In control seminiferous tubules, C14ORF39 was located in the spermatocyte nuclei and displayed linear signals in the spermatocytes with a typical sex body, which is consistent with its function as a CE component of SCs. Interestingly, the signals of the C14ORF39-M antibody were observed in the spermatocyte nuclei of individual P3907 (Figure 3D), while the C-terminal antibody signals were absent (Figure 3E), which not only reaffirmed the existence of truncated C14ORF39 but also suggested that synapsis of homologous chromosomes in individual P3907 was incomplete. Notably, spermatocytes with a typical sex body were easily found in the control, but no such cells were found in any of the available seminiferous tubules of individual P3907 carrying the homozygous *C14orf39* nonsense mutation (c.958G>T), similar to the observations in the affected individual (IV-3) from the family PK-INF-543.

For individual P6032, the identified *C14orf39* splicing mutation (c.1180−3C>G) was also expected to produce a truncated protein that was longer than that in individual P3907. To determine the localization of the truncated protein and to evaluate the synapsis of homologous chromosomes, we incubated the spermatocytes with SYCP3 and C14ORF39-M antibodies. The signals of C14ORF39-M antibody were observed as short stretches at the paired

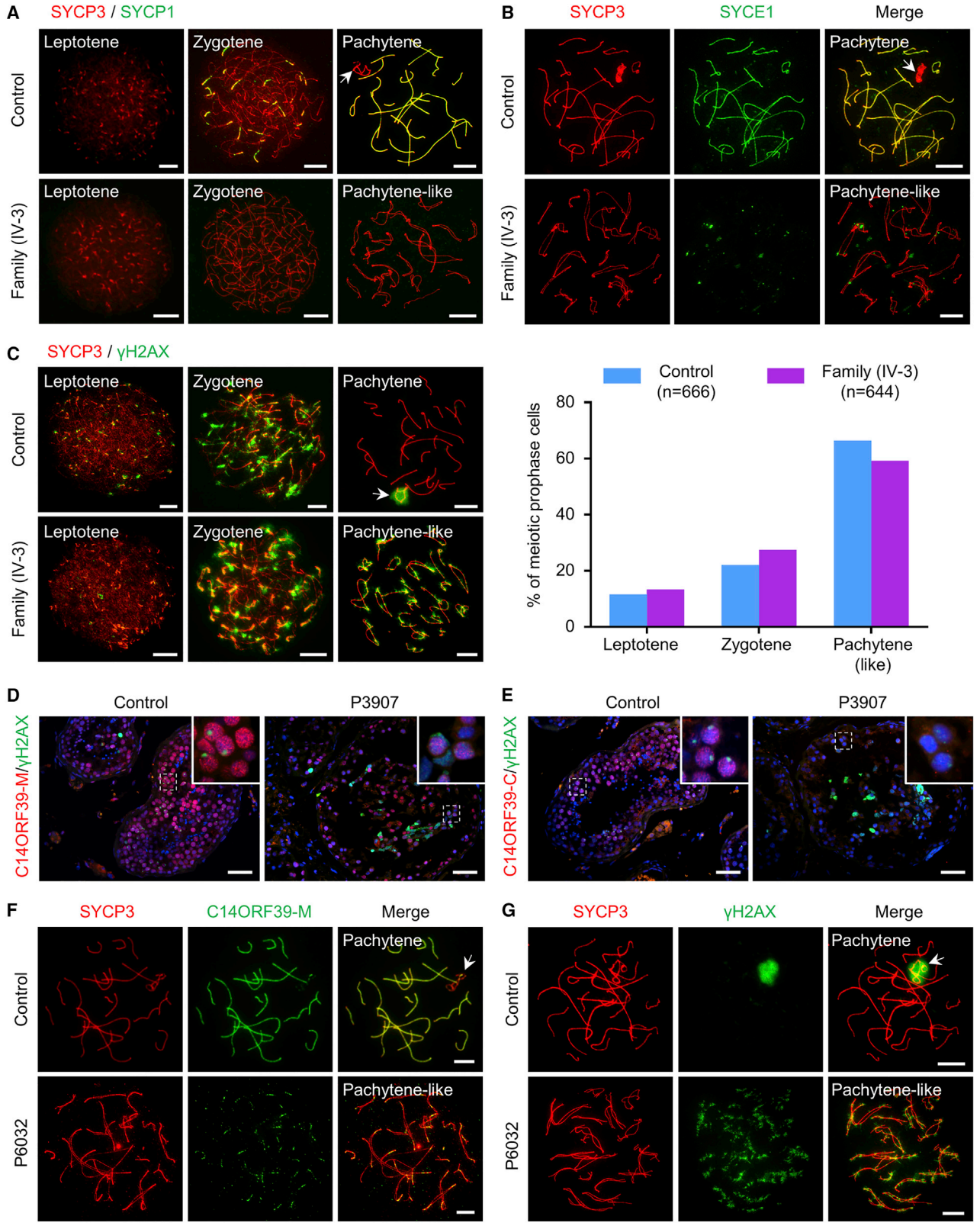

Figure 3. The spermatocytes of individuals carrying homozygous *C14orf39* mutations displayed severe synaptic defects and meiotic arrest

(A) Synapsis analyses of the spermatocytes from the control and individual IV-3 by immunofluorescence staining with antibodies against SYCP3 (red) and SYCP1 (green).

(B) Representative images of surface-spread spermatocytes from the control and individual IV-3 stained with antibodies against SYCP3 (red) and SYCE1 (green).

(legend continued on next page)

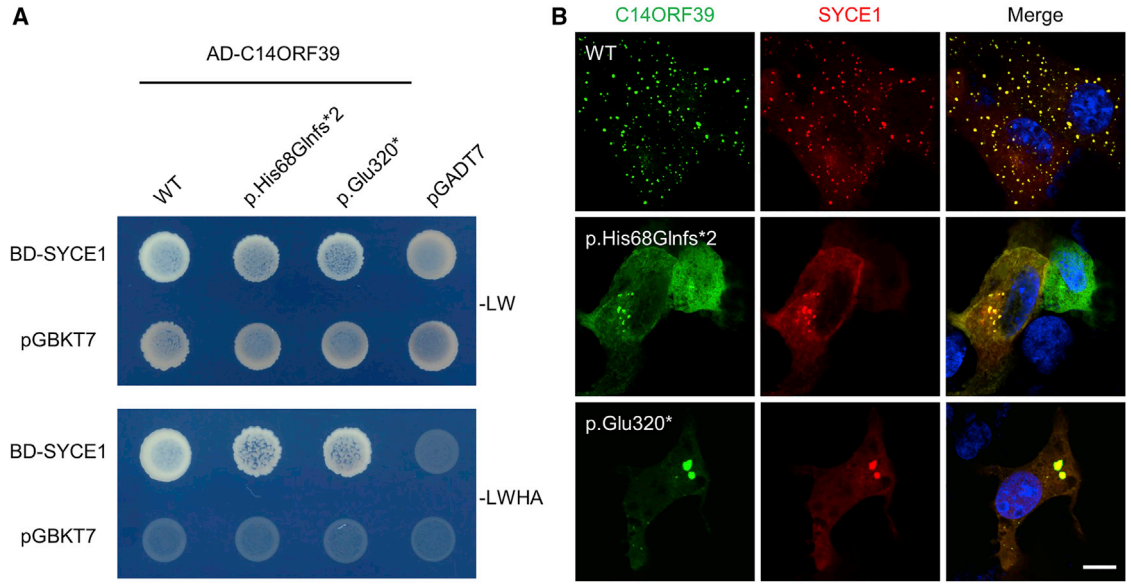

Figure 4. Mutant C14ORF39 retained SYCE1 binding but diminished polycomplex formation
(A) Yeast two-hybrid assays for pairwise protein interaction. WT and mutated C14ORF39 (p.His68Glnfs*2 and p.Glu320*) were used as prey, and mouse SYCE1 was used as bait. The pGBKT7 and pGADT7 vectors were used as negative controls. The pictures were taken after 4 days of growth. −LW, medium lacking Leu and Trp amino acids; −LWHA, medium lacking Leu, Trp, His, and Ade.
(B) Polycomplex formation assays. EGFP-fused WT and mutated C14ORF39 (green) were co-expressed with mCherry-fused SYCE1 (red) in COS-7 cells. The nuclei were stained with Hoechst 33342 (blue). The experiments were repeated three times, and the representative images are shown. Scale bars indicate 10 μm.

regions of homologous chromosomes (Figure 3F), suggesting that the truncated protein produced by the splicing mutation of *C14orf39* localized to the chromosomal axes. It bears mentioning that we never observed the C14ORF39-M signals that extended along the entire length of the autosomal axes in the spermatocytes of individual P6032, indicating incomplete synapsis in this man. Furthermore, γH2AX staining results showed that no spermatocytes were able to form a typical sex body (Figure 3G), suggesting meiotic arrest at the pachytene-like stage in this individual.

Mutant C14ORF39 retained SYCE1 binding but decreased polycomplex formation

It has been reported that C14ORF39/SIX6OS1 specifically interacts with SYCE1.[19] We thus wondered whether these mutations disrupt the interaction of C14ORF39 with SYCE1. For this purpose, we performed yeast two-hybrid (Y2H) assays to detect the protein-protein interaction (Figure 4A). Since human C14ORF39 and SYCE1 were both auto-activated in the Y2H system when used as bait, we instead used human C14ORF39 as prey and mouse SYCE1 as bait. Diploid yeast cells co-expressing Gal4-AD-fused wild-type or mutated C14ORF39 (p.His68Glnfs*2 and p.Glu320*) and Gal4-BD-fused SYCE1 grew well on the selective medium plates, suggesting that these mutations in *C14orf39* did not disrupt the interaction between C14ORF39 and SYCE1.

Because C14ORF39/SIX6OS1 can form punctate aggregates (named as polycomplex) when co-expressed with SYCE1,[19] we next examined whether these mutations affected polycomplex formation. As expected, large abundant punctate aggregates were evident in the cytoplasm of COS-7 cells that co-expressed wild-type C14ORF39 and SYCE1. Notably, the two C14ORF39 mutants (p.His68Glnfs*2 and p.Glu320*) also formed aggregates when co-expressed with SYCE1, but the number of punctate aggregates was greatly reduced (Figure 4B). These results indicated that the *C14orf39* mutations impaired polycomplex formation between C14ORF39 and SYCE1, which partly explains the synaptic defects observed in affected individuals.

(C) Meiotic prophase I analysis. Representative images of surface-spread spermatocytes from the control and individual IV-3 stained with antibodies against SYCP3 (red) and γH2AX (green). Statistical results are shown on the right side. The "n" indicates the number of meiotic prophase cells examined.
(D and E) Immunofluorescence staining of testicular sections from the control and individual P3097 with antibodies against γH2AX (green) and C14ORF39-M (D, red) or C14ORF39-C (E, red). The nuclei were stained with Hoechst 33342 (blue). The insets show magnified images of the field in white dashed rectangles. Scale bars indicate 50 μm.
(F and G) Representative images of surface-spread spermatocytes from the control and individual P6032 stained with antibodies against SYCP3 (red) and C14ORF39-M (F, green) or γH2AX (G, green). The white arrows in (A), (B), and (F) indicate sex chromosomes, and the arrows in (C) and (G) indicate the sex body. Scale bars denote 10 μm in (A), (B), (C), (F), and (G).

Six6os1 mutant mice recapitulated the NOA and POI phenotypes of individuals with homozygous *C14orf39* mutations

To confirm that the identified *C14orf39* mutations indeed cause human infertility, we characterized the phenotypes of *Six6os1* mutant mice. The *C14orf39* frameshift mutation (c.204_205del) identified in affected individuals from the consanguineous family is located at the N terminus, and the phenotypes of both male and female individuals were consistent with reported observations in *Six6os1* knockout mice.[19] Unlike the phenotype caused by the homozygous frameshift mutation (c.204_205del), the other two *C14orf39* mutations (c.958G>T and c.1180−3C>G) led to incomplete synapsis in the spermatocytes of the two affected Chinese men, possibly because of the presence of longer truncated proteins. Thus, we generated a mouse model that retained the N terminus of *Six6os1* in order to mimic that in our Chinese individuals. These mutant mice harbored a 4-bp deletion (c.907_910del [p.Asn303Serfs*9]) that did not affect *Six6os1* mRNA abundance but did lead to a truncated protein lacking 272 C-terminal amino acids, termed $Six6os1^{\Delta C/\Delta C}$ mice (Figures S4 and S5).

Two-month-old $Six6os1^{\Delta C/\Delta C}$ males showed a reduced testis size and a significant decrease ($p < 0.0001$; unpaired Student's t test; 66.3%) in the testis to body weight ratio compared to their wild-type littermates (Figures 5A and 5B). Histological analyses of testicular sections revealed no post-meiotic germ cells in the seminiferous tubules of the $Six6os1^{\Delta C/\Delta C}$ mice. In agreement with these results, no sperm were found in the epididymis of the *Six6os1* mutant mice (Figure 5C), suggesting a complete meiotic arrest.

Given that the sister (IV-5) carrying a homozygous *C14orf39* mutation was diagnosed with POI, we thus analyzed the ovaries of 3-days-postpartum (dpp) and 10-week-old female mice histopathologically. We easily detected numerous follicles of different developmental stages in the ovarian sections of wild-type mice. However, no follicles were found in the female *Six6os1* mutant mice at each age examined (Figure 5D). Furthermore, the serum AMH levels of 3- to 4-month-old $Six6os1^{\Delta C/\Delta C}$ female mice averaged 0.22 ng/mL, significantly lower than that in wild-type mice, which showed an average serum AMH level of 28.57 ng/mL ($p < 0.001$; Welch's t test; Figure 5E). These results suggested that $Six6os1^{\Delta C/\Delta C}$ female mice mimicked the POI phenotype of the affected sister.

To identify the exact substage at which meiotic arrest occurred in $Six6os1^{\Delta C/\Delta C}$ male mice, we examined the progression of meiotic prophase I, as we did for the affected individuals. In wild-type spermatocytes, γH2AX signals that were diffused in the nuclei at leptotene gradually diminished as synapsis ensued during zygotene and finally disappeared from autosomes. The γH2AX signals ultimately accumulated on sex chromosomes to form the sex body from the pachytene to diplotene stage. However, in *Six6os1* mutant spermatocytes, γH2AX signals appeared and diminished normally but were persistent on the chromosomes and failed to form the sex body, thereby indicating a meiotic arrest, as observed in the affected men (Figure 6A). Next, we investigated the chromosomal synapsis by staining the spermatocytes with antibodies against SYCP3 and SYCP1. In wild-type pachytene spermatocytes, SYCP1 showed a continuous linear signal along the entire length of the autosomal axes. However, only short stretches of SYCP1 signals were observable in the most advanced spermatocytes of $Six6os1^{\Delta C/\Delta C}$ mice (Figure 6B). Similar results were observed for another synapsis marker, SYCE1 (Figure 6C), further indicating that the homologous chromosomes underwent incomplete synapsis in the mutant mice. Considering the essential role of SIX6OS1 in synapsis initiation, we inferred that the truncated SIX6OS1 should be located on the chromosomal axes. To test this, we stained the surface-spread spermatocytes with antibodies against SYCP3 and the N terminus of SIX6OS1 (SIX6OS1-N). In agreement with our presumption, the SIX6OS1 threads were detected in the synapsed regions of homologous chromosomes in *Six6os1* mutant spermatocytes (Figure 6D). Taken together, these results showed that $Six6os1^{\Delta C/\Delta C}$ male mice recapitulated the NOA phenotype found in the affected men.

Discussion

SC is essential for crossover formation between homologous chromosomes and the successful production of gametes in mammals. The deficiency of SC components in mice consistently results in infertility or subfertility.[14–19] Here, for the first time, we identified three homozygous variants in *C14orf39* from both male and female infertile individuals. All of these *C14orf39* mutations led to severe synaptic defects and meiotic arrest in affected individuals, which was strongly supported by the observations in our *Six6os1* (the murine ortholog of human *C14orf39*) mutant mice that recapitulated the phenotypes of our NOA- and POI-affected individuals, as well as in previously reported *Six6os1* knockout mice.[19] Our results thus confirm an important and conserved role for C14ORF39/SIX6OS1 in chromosomal synapsis and demonstrate that mutations in *C14orf39* can result in human infertility.

The N terminus of C14ORF39/SIX6OS1 contains two SYCE1 binding regions: one located at the amino acid region from residues 1–67 and the other from 68–267. The integrity of the two SIX6OS1-SYCE1 binding interfaces is essential for SC assembly *in vivo*.[39] The *C14orf39* frameshift mutation (c.204_205del [p.His68Glnfs*2]) retains the first but loses the second binding interface and thus adversely affects protein function. Consistent with this finding, the mutant protein can still interact with SYCE1, but its ability to form aggregates with SYCE1 is diminished. More importantly, individuals with this frameshift mutation showed complete asynapsis of homologous chromosomes, confirming the pathogenicity of this mutation. Additionally,

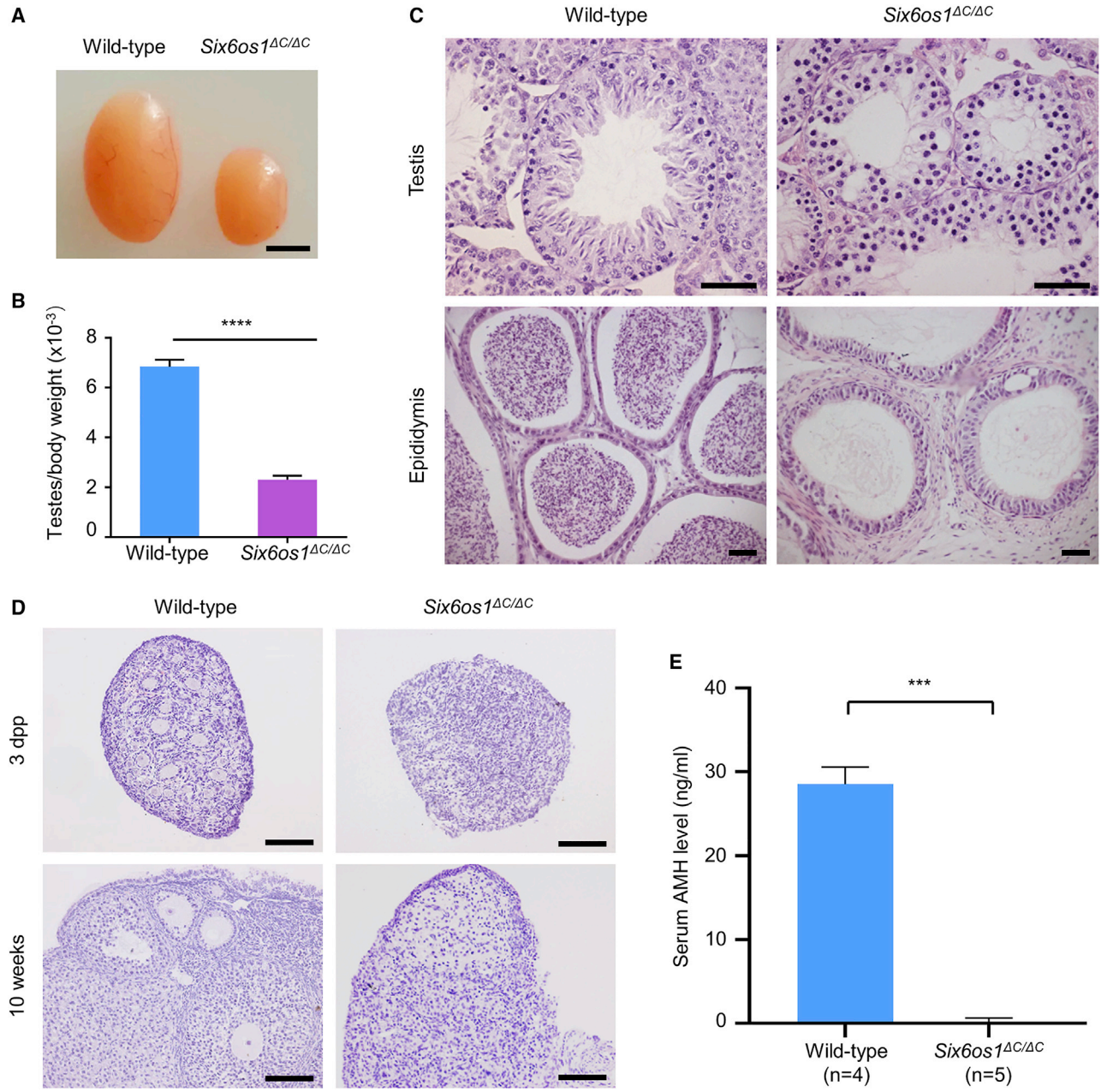

Figure 5. *Six6os1*$^{\Delta C/\Delta C}$ mice recapitulated the NOA and POI phenotypes of individuals with homozygous *C14orf39* mutations
(A) Testis morphology of 2-month-old wild-type and *Six6os1*$^{\Delta C/\Delta C}$ mice. Scale bar indicates 2 mm.
(B) Testis to body weight ratio. The data are obtained from three mice for each genotype and represent means ± SD. The significance was determined via unpaired Student's t test. ****$p < 0.0001$.
(C) Histological sections of testes and epididymides from wild-type and *Six6os1*$^{\Delta C/\Delta C}$ mice. Scale bars denote 50 μm.
(D) Histological sections of ovaries from wild-type and *Six6os1*$^{\Delta C/\Delta C}$ female mice at the indicated ages were stained with hematoxylin. Scale bars indicate 50 μm.
(E) The serum AMH levels of 3- to 4-month-old wild-type and *Six6os1*$^{\Delta C/\Delta C}$ female mice. Data are expressed as means ± SD, and n shows the number of mice analyzed. Welch's t test was used to determine statistical significance. ***$p < 0.001$. AMH, anti-Müllerian hormone.

our *in vitro* and *in vivo* studies showed that both the *C14orf39* nonsense mutation (c.958G>T [p.Glu320*]) and splicing mutation (c.1180−3C>G) resulted in the generation of truncated proteins. Interestingly, although the two binding interfaces are retained, the mutant C14ORF39 protein (p.Glu320*) also displayed an impaired polycomplex formation between C14ORF39 and SYCE1 in COS-7 cells. Furthermore, the individuals carrying these two homozygous *C14orf39* mutations also exhibited synaptic defects and meiotic arrest, thereby providing *in vivo* evidence for the pathogenicity of these two mutations.

Previous study has shown that homologous chromosomes are unable to synapse in *Six6os1* knockout mice.[19] In contrast, the homologous chromosomes

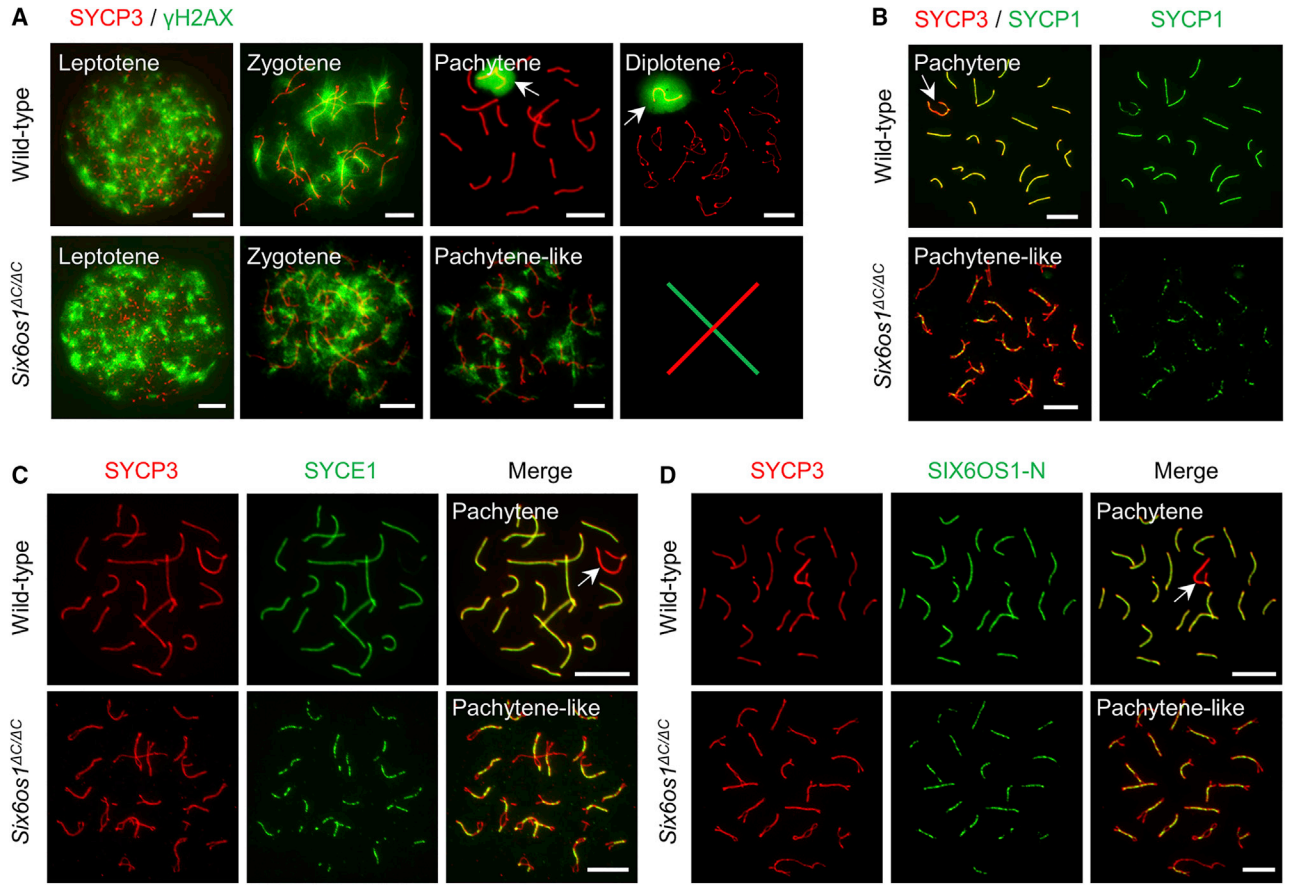

Figure 6. *Six6os1*$^{\Delta C/\Delta C}$ male mice displayed meiotic arrest and incomplete synapsis between homologous chromosomes

(A) The progression of meiotic prophase I was analyzed by immunostaining surface-spread spermatocytes from wild-type and *Six6os1*$^{\Delta C/\Delta C}$ mice with antibodies against SYCP3 (red) and γH2AX (green). Representative images of leptotene, zygotene, pachytene, and diplotene spermatocytes from wild-type mice are shown. The meiosis of *Six6os1*$^{\Delta C/\Delta C}$ mice was arrested at the pachytene-like stage. (B and C) Immunofluorescence staining of surface-spread spermatocytes from wild-type and *Six6os1*$^{\Delta C/\Delta C}$ mice with antibodies against SYCP3 (red) and SYCP1 (B, green) or SYCE1 (C, green).

(D) Representative images of surface-spread spermatocytes from wild-type and *Six6os1*$^{\Delta C/\Delta C}$ mice stained with antibodies against SYCP3 (red) and SIX6OS1-N (green). The white arrows in (A) indicate the sex body, and the arrows in (B), (C), and (D) indicate sex chromosomes. Scale bars denote 10 μm.

undergo partial synapsis in some closely co-aligned regions in our *Six6os1*$^{\Delta C/\Delta C}$ mice. These phenotypic differences are also observed between our Pakistani and Chinese affected individuals, indicating that the N terminus of C14ORF39/SIX6OS1 is sufficient to interact with SYCE1 and forms a complex with SYCE3 and SYCP1,[17,40] thereby initiating SC assembly. Furthermore, the incomplete synapsis in *Six6os1*$^{\Delta C/\Delta C}$ mice is reminiscent of *Syce2* and *Tex12* knockout mice,[16,18] suggesting that the C terminus of C14ORF39/SIX6OS1 plays an indispensable role in facilitating SC extension along the entire chromosomal axes.

It is worth noting that these three homozygous mutations in *C14orf39* are identified from different ethnic populations. The first *C14orf39* frameshift mutation was found in one of 50 Pakistani consanguineous families with at least two infertile siblings in each, which accounts for 2% of familial infertility. The other two *C14orf39* mutations (one nonsense mutation and one splicing mutation) were found in two of 60 infertile Chinese men with meiotic arrest. In addition, a missense variant (p.Leu524-Phe) in *C14orf39* has been associated with higher recombination rates in human females in the Icelandic population.[26] These results indicate that mutations in *C14orf39* are not rare and are closely linked with human infertility, and individuals with NOA or POI should undertake mutation screening of *C14orf39*.

To date, several mutations in SC components have been reported to be associated with human infertility.[22–25] Notably, the mutations in *C14orf39* we identified and the previously reported *SYCE1* mutations are all homozygous and segregate with the disease via an autosomal recessive inheritance. However, *SYCP3* and *SYCP2* heterozygous mutations are also reported in azoospermic men or women with recurrent pregnancy loss and probably display a dominant-negative effect.[24,41] These cases suggest that in human infertility, mutations occur frequently in the SC-coding genes and screening for mutations in these genes should be considered for adoption in the clinical practice of human-assisted reproduction.

In conclusion, our present data demonstrate that homozygous mutations in *C14orf39* cause severe synaptic defects and meiotic arrest, which consequently leads to NOA and POI in humans. These findings highlight the essential and conserved role of C14ORF39/SIX6OS1 in SC assembly and will facilitate genetic diagnoses for clinical infertility while also enabling development of possible treatments for infertile individuals in the future.

Data and code availability

The accession numbers for the *C14orf39* variants reported in this paper are ClinVar: SCV001468897, SCV001468898, and SCV001468899. The WES datasets supporting the current study have not been deposited in a public repository because of privacy and ethical restrictions but are available from the corresponding authors on request. The relevant NCBI accession numbers are GenBank: NM_174978.3 (for the reference sequence of human *C14orf39*), NP_777638.3 (for the reference sequence of human C14ORF39 protein), and NM_029444.2 (for the reference sequence of mouse *Six6os1*).

Supplemental Information

Supplemental Information can be found online at https://doi.org/10.1016/j.ajhg.2021.01.010.

Acknowledgments

We are very grateful to all individuals for their informed consent to donate their DNA and tissue biopsies for scientific research and to the physicians who take care of them. This work was supported by the National Natural Science Foundation of China (31630050, 31890780, 32061143006, 31871514, and 82071709), the National Key Research and Developmental Program of China (2016YFC1000600, 2018YFC1003700, and 2018YFC1003900), the Strategic Priority Research Program of the Chinese Academy of Sciences (XDB19000000), and the Fundamental Research Funds for the Central Universities (YD2070002006 and WK9100000004).

Declaration of interests

The authors declare no competing interests.

Received: October 23, 2020
Accepted: January 11, 2021
Published: January 27, 2021

Web resources

1000 Genomes Project, https://www.internationalgenome.org/home
COILS, https://embnet.vital-it.ch/software/COILS_form.html
ESP6500, https://evs.gs.washington.edu/EVS/
gnomAD, https://gnomad.broadinstitute.org/
OMIM, https://omim.org/
RefSeq, https://www.ncbi.nlm.nih.gov/refseq/
SpermatogenesisOnline 1.0, https://mcg.ustc.edu.cn/bsc/spermgenes/

References

1. Zegers-Hochschild, F., Adamson, G.D., de Mouzon, J., Ishihara, O., Mansour, R., Nygren, K., Sullivan, E., Vanderpoel, S.; International Committee for Monitoring Assisted Reproductive Technology; and World Health Organization (2009). International Committee for Monitoring Assisted Reproductive Technology (ICMART) and the World Health Organization (WHO) revised glossary of ART terminology, 2009. Fertil. Steril. *92*, 1520–1524.
2. Vander Borght, M., and Wyns, C. (2018). Fertility and infertility: Definition and epidemiology. Clin. Biochem. *62*, 2–10.
3. Krausz, C., Cioppi, F., and Riera-Escamilla, A. (2018). Testing for genetic contributions to infertility: potential clinical impact. Expert Rev. Mol. Diagn. *18*, 331–346.
4. Zorrilla, M., and Yatsenko, A.N. (2013). The Genetics of Infertility: Current Status of the Field. Curr. Genet. Med. Rep. *1*, 247–260.
5. Caburet, S., Arboleda, V.A., Llano, E., Overbeek, P.A., Barbero, J.L., Oka, K., Harrison, W., Vaiman, D., Ben-Neriah, Z., García-Tuñón, I., et al. (2014). Mutant cohesin in premature ovarian failure. N. Engl. J. Med. *370*, 943–949.
6. Weinberg-Shukron, A., Rachmiel, M., Renbaum, P., Gulsuner, S., Walsh, T., Lobel, O., Dreifuss, A., Ben-Moshe, A., Zeligson, S., Segel, R., et al. (2018). Essential Role of BRCA2 in Ovarian Development and Function. N. Engl. J. Med. *379*, 1042–1049.
7. Qin, Y., Zhang, F., and Chen, Z.J. (2019). BRCA2 in Ovarian Development and Function. N. Engl. J. Med. *380*, 1086.
8. Yatsenko, A.N., Georgiadis, A.P., Röpke, A., Berman, A.J., Jaffe, T., Olszewska, M., Westernströer, B., Sanfilippo, J., Kurpisz, M., Rajkovic, A., et al. (2015). X-linked TEX11 mutations, meiotic arrest, and azoospermia in infertile men. N. Engl. J. Med. *372*, 2097–2107.
9. Yang, F., Silber, S., Leu, N.A., Oates, R.D., Marszalek, J.D., Skaletsky, H., Brown, L.G., Rozen, S., Page, D.C., and Wang, P.J. (2015). TEX11 is mutated in infertile men with azoospermia and regulates genome-wide recombination rates in mouse. EMBO Mol. Med. *7*, 1198–1210.
10. Wang, J., Zhang, W., Jiang, H., Wu, B.L.; and Primary Ovarian Insufficiency Collaboration (2014). Mutations in HFM1 in recessive primary ovarian insufficiency. N. Engl. J. Med. *370*, 972–974.
11. Yao, C., Yang, C., Zhao, L., Li, P., Tian, R., Chen, H., et al. (2020). Bi-allelic *SHOC1* loss-of-function mutations cause meiotic arrest and non-obstructive azoospermia. J. Med. Genet. https://doi.org/10.1136/jmedgenet-2020-107042.
12. Matzuk, M.M., and Lamb, D.J. (2008). The biology of infertility: research advances and clinical challenges. Nat. Med. *14*, 1197–1213.
13. Gao, J., and Colaiácovo, M.P. (2018). Zipping and Unzipping: Protein Modifications Regulating Synaptonemal Complex Dynamics. Trends Genet. *34*, 232–245.
14. de Vries, F.A., de Boer, E., van den Bosch, M., Baarends, W.M., Ooms, M., Yuan, L., Liu, J.G., van Zeeland, A.A., Heyting, C., and Pastink, A. (2005). Mouse Sycp1 functions in synaptonemal complex assembly, meiotic recombination, and XY body formation. Genes Dev. *19*, 1376–1389.
15. Bolcun-Filas, E., Hall, E., Speed, R., Taggart, M., Grey, C., de Massy, B., Benavente, R., and Cooke, H.J. (2009). Mutation of the mouse Syce1 gene disrupts synapsis and suggests a link between synaptonemal complex structural components and DNA repair. PLoS Genet. *5*, e1000393.

16. Bolcun-Filas, E., Costa, Y., Speed, R., Taggart, M., Benavente, R., De Rooij, D.G., and Cooke, H.J. (2007). SYCE2 is required for synaptonemal complex assembly, double strand break repair, and homologous recombination. J. Cell Biol. *176*, 741–747.
17. Schramm, S., Fraune, J., Naumann, R., Hernandez-Hernandez, A., Höög, C., Cooke, H.J., Alsheimer, M., and Benavente, R. (2011). A novel mouse synaptonemal complex protein is essential for loading of central element proteins, recombination, and fertility. PLoS Genet. *7*, e1002088.
18. Hamer, G., Wang, H., Bolcun-Filas, E., Cooke, H.J., Benavente, R., and Höög, C. (2008). Progression of meiotic recombination requires structural maturation of the central element of the synaptonemal complex. J. Cell Sci. *121*, 2445–2451.
19. Gómez-H, L., Felipe-Medina, N., Sánchez-Martín, M., Davies, O.R., Ramos, I., García-Tuñón, I., de Rooij, D.G., Dereli, I., Tóth, A., Barbero, J.L., et al. (2016). C14ORF39/SIX6OS1 is a constituent of the synaptonemal complex and is essential for mouse fertility. Nat. Commun. *7*, 13298.
20. Yuan, L., Liu, J.G., Zhao, J., Brundell, E., Daneholt, B., and Höög, C. (2000). The murine SCP3 gene is required for synaptonemal complex assembly, chromosome synapsis, and male fertility. Mol. Cell *5*, 73–83.
21. Yang, F., De La Fuente, R., Leu, N.A., Baumann, C., McLaughlin, K.J., and Wang, P.J. (2006). Mouse SYCP2 is required for synaptonemal complex assembly and chromosomal synapsis during male meiosis. J. Cell Biol. *173*, 497–507.
22. Geisinger, A., and Benavente, R. (2016). Mutations in Genes Coding for Synaptonemal Complex Proteins and Their Impact on Human Fertility. Cytogenet. Genome Res. *150*, 77–85.
23. Pashaei, M., Rahimi Bidgoli, M.M., Zare-Abdollahi, D., Najmabadi, H., Haji-Seyed-Javadi, R., Fatehi, F., and Alavi, A. (2020). The second mutation of SYCE1 gene associated with autosomal recessive nonobstructive azoospermia. J. Assist. Reprod. Genet. *37*, 451–458.
24. Schilit, S.L.P., Menon, S., Friedrich, C., Kammin, T., Wilch, E., Hanscom, C., Jiang, S., Kliesch, S., Talkowski, M.E., Tüttelmann, F., et al. (2020). SYCP2 Translocation-Mediated Dysregulation and Frameshift Variants Cause Human Male Infertility. Am. J. Hum. Genet. *106*, 41–57.
25. Hernández-López, D., Geisinger, A., Trovero, M.F., Santiñaque, F.F., Brauer, M., Folle, G.A., Benavente, R., and Rodríguez-Casuriaga, R. (2020). Familial primary ovarian insufficiency associated with an SYCE1 point mutation: defective meiosis elucidated in humanized mice. Mol. Hum. Reprod. *26*, 485–497.
26. Kong, A., Thorleifsson, G., Frigge, M.L., Masson, G., Gudbjartsson, D.F., Villemoes, R., Magnusdottir, E., Olafsdottir, S.B., Thorsteinsdottir, U., and Stefansson, K. (2014). Common and low-frequency variants associated with genome-wide recombination rate. Nat. Genet. *46*, 11–16.
27. Begum, F., Chowdhury, R., Cheung, V.G., Sherman, S.L., and Feingold, E. (2016). Genome-Wide Association Study of Meiotic Recombination Phenotypes. G3 (Bethesda) *6*, 3995–4007.
28. World Health Organization (2010). WHO laboratory manual for the examination and processing of human semen (New York: World Health Organization).
29. Yin, H., Ma, H., Hussain, S., Zhang, H., Xie, X., Jiang, L., Jiang, X., Iqbal, F., Bukhari, I., Jiang, H., et al. (2019). A homozygous FANCM frameshift pathogenic variant causes male infertility. Genet. Med. *21*, 62–70.
30. Nyholt, D.R. (2000). All LODs are not created equal. Am. J. Hum. Genet. *67*, 282–288.
31. Wang, K., Li, M., and Hakonarson, H. (2010). ANNOVAR: functional annotation of genetic variants from high-throughput sequencing data. Nucleic Acids Res. *38*, e164.
32. Zhang, Y., Zhong, L., Xu, B., Yang, Y., Ban, R., Zhu, J., Cooke, H.J., Hao, Q., and Shi, Q. (2013). SpermatogenesisOnline 1.0: a resource for spermatogenesis based on manual literature curation and genome-wide data mining. Nucleic Acids Res. *41*, D1055–D1062.
33. Jiao, Y., Fan, S., Jabeen, N., Zhang, H., Khan, R., Murtaza, G., et al. (2020). A TOP6BL mutation abolishes meiotic DNA double-strand break formation and causes human infertility. Sci. Bull. *65*, 2120–2129.
34. Peters, A.H., Plug, A.W., van Vugt, M.J., and de Boer, P. (1997). A drying-down technique for the spreading of mammalian meiocytes from the male and female germline. Chromosome Res. *5*, 66–68.
35. Jiang, X., Yin, S., Fan, S., Bao, J., Jiao, Y., Ali, A., Iqbal, F., Xu, J., Zhang, Y., and Shi, Q. (2019). *Npat*-dependent programmed Sertoli cell proliferation is indispensable for testis cord development and germ cell mitotic arrest. FASEB J. *33*, 9075–9086.
36. Qin, Y., Jiao, X., Simpson, J.L., and Chen, Z.J. (2015). Genetics of primary ovarian insufficiency: new developments and opportunities. Hum. Reprod. Update *21*, 787–808.
37. Subramanian, V.V., and Hochwagen, A. (2014). The meiotic checkpoint network: step-by-step through meiotic prophase. Cold Spring Harb. Perspect. Biol. *6*, a016675.
38. Li, J., Leng, M., Ma, T., Yu, D., Shi, H., and Shi, Q. (2009). Cryopreservation has no effect on meiotic recombination and synapsis in testicular tissues. Fertil. Steril. *91* (4, Suppl), 1404–1407.
39. Sanchez-Saez, F., Gomez, H.L., Dunne, O.M., Gallego-Paramo, C., Felipe-Medina, N., Sanchez-Martin, M., Llano, E., Pendas, A.M., and Davies, O.R. (2020). Meiotic chromosome synapsis depends on multivalent SYCE1-SIX6OS1 interactions that are disrupted in cases of human infertility. Sci. Adv. *6*, eabb1660.
40. Lu, J., Gu, Y., Feng, J., Zhou, W., Yang, X., and Shen, Y. (2014). Structural insight into the central element assembly of the synaptonemal complex. Sci. Rep. *4*, 7059.
41. Bolor, H., Mori, T., Nishiyama, S., Ito, Y., Hosoba, E., Inagaki, H., Kogo, H., Ohye, T., Tsutsumi, M., Kato, T., et al. (2009). Mutations of the SYCP3 gene in women with recurrent pregnancy loss. Am. J. Hum. Genet. *84*, 14–20.

The American Journal of Human Genetics, Volume *108*

Supplemental Data

Homozygous mutations in *C14orf39*/*SIX6OS1* cause non-obstructive azoospermia and premature ovarian insufficiency in humans

Suixing Fan, Yuying Jiao, Ranjha Khan, Xiaohua Jiang, Abdul Rafay Javed, Asim Ali, Huan Zhang, Jianteng Zhou, Muhammad Naeem, Ghulam Murtaza, Yang Li, Gang Yang, Qumar Zaman, Muhammad Zubair, Haiyang Guan, Xingxia Zhang, Hui Ma, Hanwei Jiang, Haider Ali, Sobia Dil, Wasim Shah, Niaz Ahmad, Yuanwei Zhang, and Qinghua Shi

Supplemental Note: Case Reports

The two affected males (IV-2 and IV-3) in the family PK-INF-543 were 40 and 37 years old (Figure 1A), respectively. They had normal height and body weight and had no other serious diseases except suffered from primary infertility. At least two semen analyses indicated that they had normal semen volume but no sperm, and reproductive hormone levels within the normal range (Table 1). After obtaining informed consent, we obtained a testicular biopsy from individual IV-3 and performed H&E staining on the testicular sections. For the control, many spermatogenic cells including spermatogonia, spermatocytes, and spermatozoa were observed in the seminiferous tubules, but for individual IV-3, spermatogonia and spermatocytes were found, but post-meiotic cells were absent (Figure 1B). These results suggested that the affected males (IV-2 and IV-3) in this family were individuals with NOA. The father (III-1) and mother (III-2) in this family were first cousins. Their siblings married outside of the family, and each has multiple children with no history of infertility. The unaffected married brothers (IV-1 and IV-4) of the proband (IV-2) were fertile and fathered five and one offspring, respectively. The other two brothers (IV-6 and IV-7, 28 and 24 years old, respectively) and one sister (IV-5, 30 years old) were unmarried with unknown fertility status. Cytogenetic studies indicated that all the affected individuals, their siblings, and mother had normal karyotypes (Table 1).

For the unmarried sister (IV-5) in this Pakistani family, we noticed that the levels of her reproductive hormones were abnormal (Table 1). Specifically, she had elevated

levels of follicle-stimulating hormone (FSH, 49.06 mIU/ml) and luteinizing hormone (LH, 47.69 mIU/ml), as well as dramatically reduced levels of anti-Müllerian hormone (AMH, 0.021 ng/ml). This sister had menarche at the age of 17, followed by a history of irregular menstrual cycles, and reached menopause at the age of 24. Furthermore, her uterus and ovaries were small, with the left ovary being smooth and without follicular activity; in the expected location of the right ovary, there was only a small cyst (18 mm). These features indicated that the sister (IV-5) suffered from POI.[1]

The two affected Chinese men (P3907 and P6032) were 37 and 30 years old, respectively (Figure 1A). Individual P3907 was born into a consanguineous marriage. However, his parents were unwilling to provide blood samples. These two individuals also had normal karyotypes (46, XY) and no Y-chromosome microdeletions, but no sperm in their semen. Through histological examination of their testicular sections, we found no spermatozoa in the seminiferous tubules (Figure 1B).

Supplemental Figures

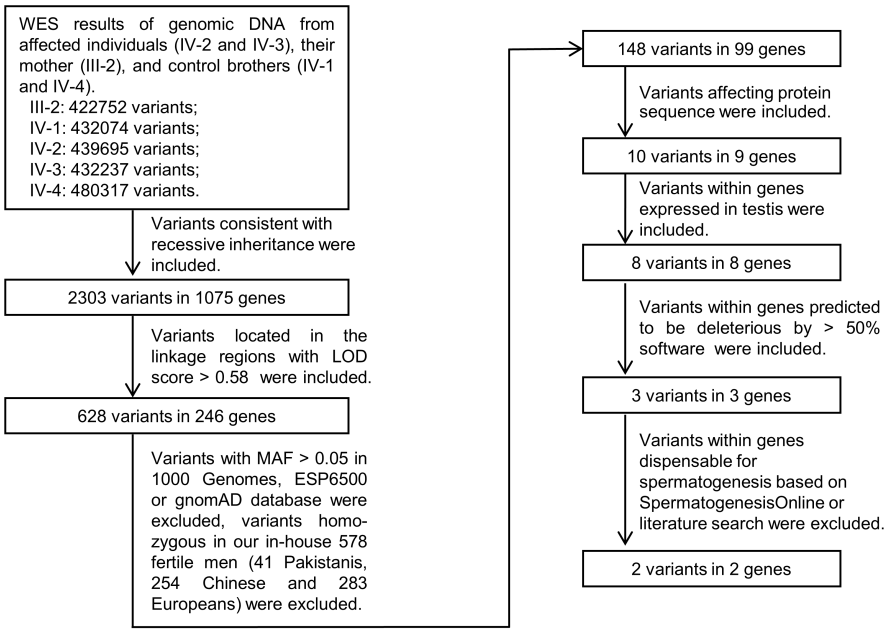

Figure S1. The workflow for whole-exome sequencing data analysis

The flowchart shows the strategy to filter the candidate variants for the Pakistani family. LOD, the logarithm of the odds; WES, whole-exome sequencing; MAF, minor allele frequency.

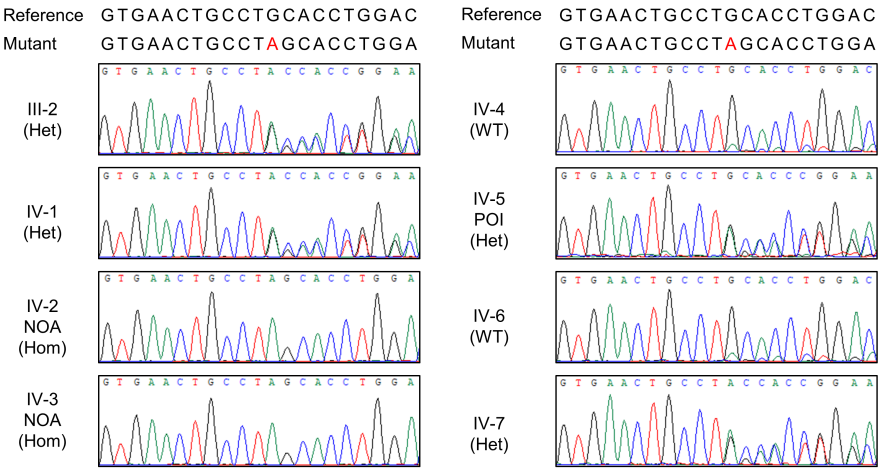

Figure S2. Detection of *DHRS4L2* variant by Sanger sequencing in all available family members

Genomic DNA extracted from peripheral blood was used as the PCR template to detect the variant (1-bp insertion) in *DHRS4L2*. The two brothers with NOA are homozygous for *DHRS4L2* mutation, but the sister (IV-5) who was diagnosed with POI carries a heterozygous *DHRS4L2* mutation, as is identified in her mother (III-2). Other unaffected family members are either heterozygous or wild type (WT). Hom, homozygous; Het, heterozygous; NOA, non-obstructive azoospermia; POI, premature ovarian insufficiency.

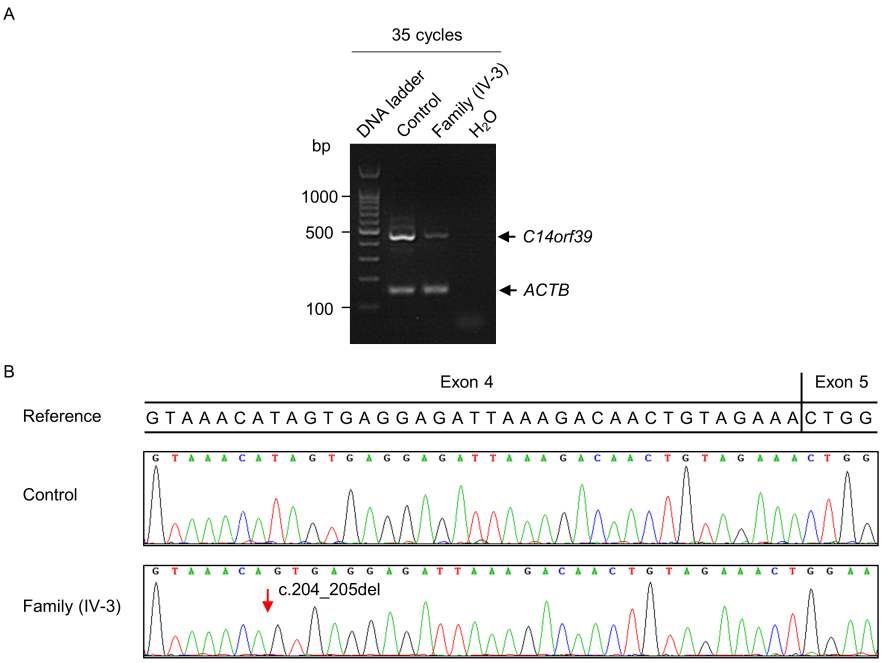

Figure S3. Detection of *C14orf39* mutation at the cDNA level by RT-PCR and Sanger sequencing

(**A**) The total RNAs extracted from the testicular tissues of a man with obstructive azoospermia and individual IV-3 were used to synthesize the cDNAs by RT-PCR. *C14orf39* and *ACTB* primer pairs were added simultaneously in the PCR mixture. The *C14orf39* band can be observed under 35 cycles of amplification in both control and individual IV-3. *ACTB* was used as an internal control. (**B**) Sanger sequencing chromatograms of testicular cDNAs of control and the individual IV-3. The red arrow indicates the 2-bp deletion in *C14orf39*.

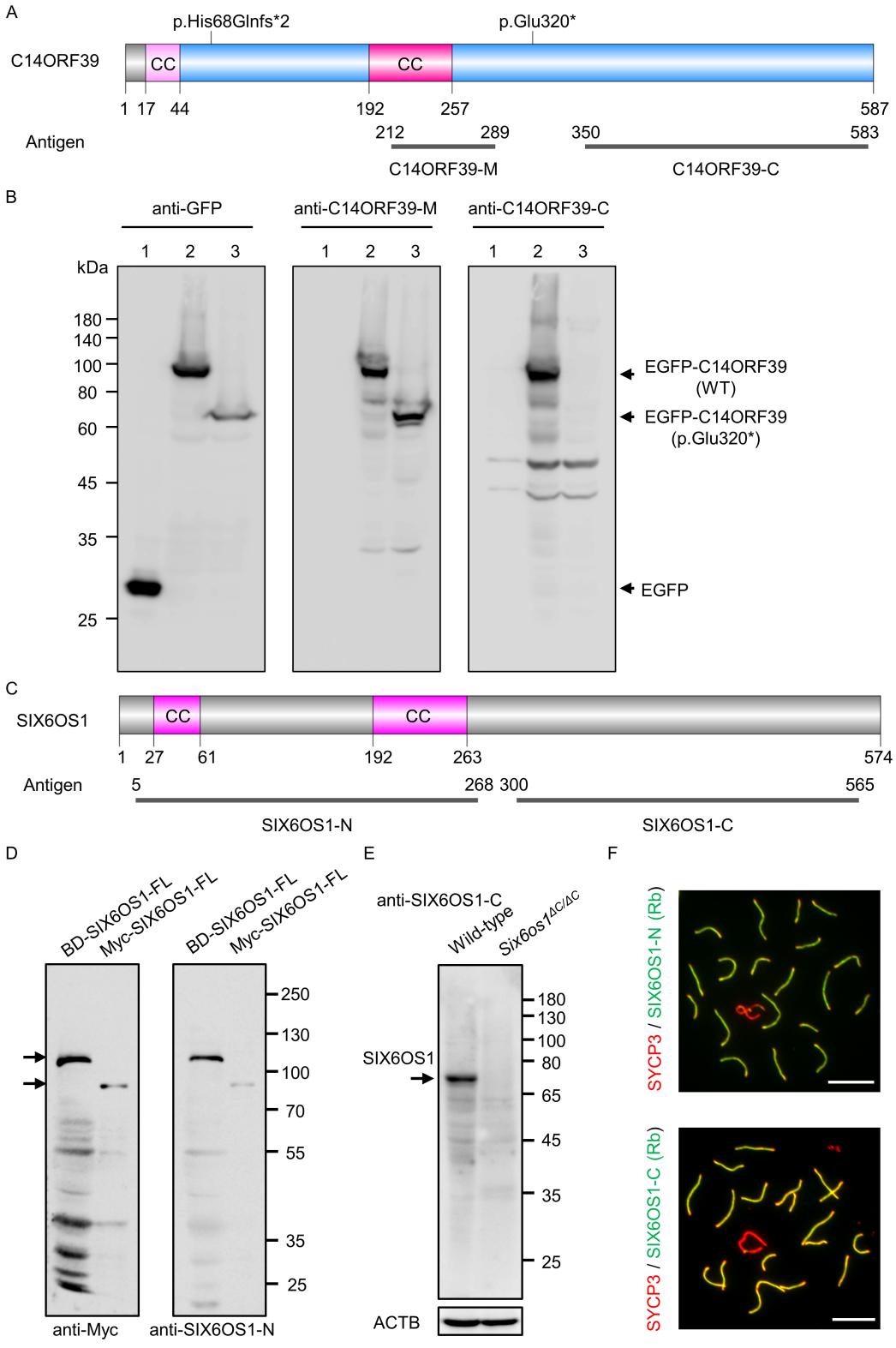

Figure S4. Validation of human C14ORF39 and mouse SIX6OS1 antibodies

(**A**) Schematic representation of the antigen information about human C14ORF39 antibodies. (**B**) Validation of C14ORF39 antibodies by Western blot. The whole-cell

lysates were extracted from transfected HEK293T cells. Lane 1: EGFP; lane 2: EGFP-C14ORF39; lane 3: EGFP-C14ORF39-E320X. Wild-type and mutated C14ORF39 fusion proteins were detected by C14ORF39-M and –C antibodies. The GFP antibody was used as a positive control. The arrows indicate the target proteins. (**C**) Schematic representation of the antigen information about the antibodies against SIX6OS1-N and SIX6OS1-C. Two putative coiled-coil domains (CC, pink) are indicated in the SIX6OS1 protein. (**D**) Validation of C14ORF39-N antibody by Western blot. Gal4-DNA binding domain tagged SIX6OS1 protein (BD-SIX6OS1-FL) was obtained from the transformed yeast cells, and Myc-tagged SIX6OS1 protein was extracted from the transfected HEK293T cells. The Myc antibody was used as a positive control. (**E**) Validation of C14ORF39-C antibody by Western blot. Testicular lysates were obtained from wild-type and *Six6os1*$^{\Delta C/\Delta C}$ mice at 16 dpp. ACTB was used as an internal control. Arrows indicate the target proteins. (**F**) Immunofluorescence staining of surface-spread spermatocytes from 10-week-old wild-type mice using SYCP3 (red) and different SIX6OS1 antibodies (green). Rb, rabbit. Scale bars denote 10 μm.

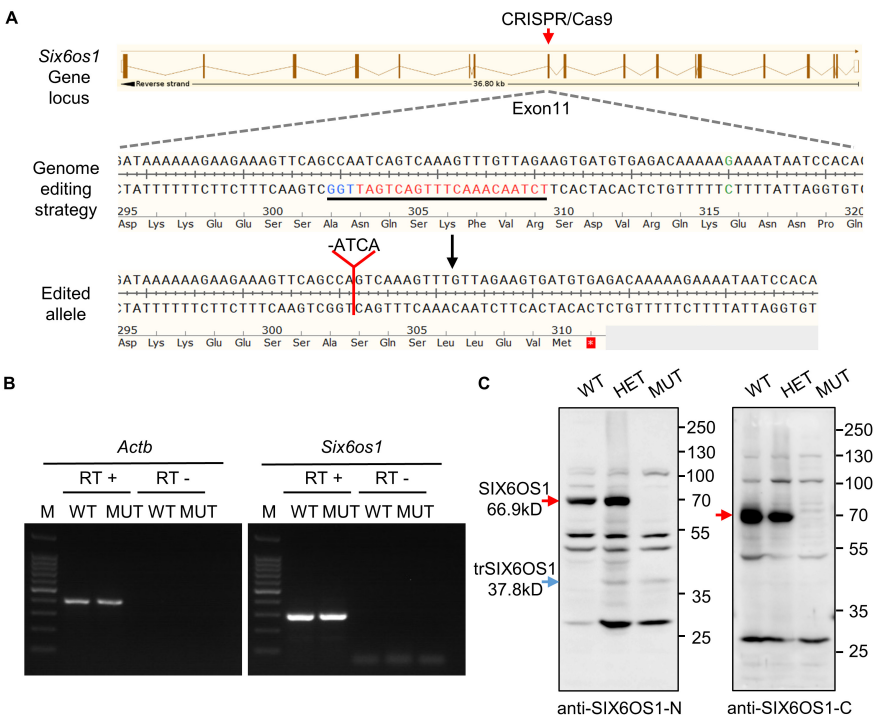

Figure S5. Generation and verification of the *Six6os1*$^{\Delta C/\Delta C}$ mouse model

(**A**) The strategy for the generation of *Six6os1*$^{\Delta C/\Delta C}$ mice by CRISPR/Cas9 technology. The colored nucleotides with a black line indicate the single guide RNA (sgRNA) targeting sequence. Four base pair deletion introduces a premature stop codon (red asterisk). (**B**) The expression of *Six6os1* was evaluated by RT-PCR in testes of 10-week-old WT and *Six6os1*$^{\Delta C/\Delta C}$ mice. *Actb* was served as internal control and underwent 28 cycles of amplification. *Six6os1* was amplified for 35 cycles. RT+, with reverse transcriptase; RT-, without reverse transcriptase. (**C**) Detection of SIX6OS1 protein from the testis lysates of 16 dpp mice by Western blot using antibodies against the N-terminal and C-terminal of SIX6OS1, respectively. Red arrows indicate the full-length SIX6OS1 and blue arrow indicates the truncated SIX6OS1 (trSIX6OS1). WT, wild-type; HET, heterozygous; MUT, homozygous.

Supplemental Tables

Table S1. The antibodies used in this study

Primary antibodies				
Target	**Dilution**	**Host species**	**Supplier**	**Catalog number**
Human SYCP3	1:200	Mouse	Proteintech	66409-1-Ig
Human SYCP1	1:80	Rabbit	Novus Biologicals	NB300-228
Human SYCE1	1:50	Rabbit	Proteintech	11063-1-AP
Human C14ORF39-M	1:50	Rabbit	Novus Biologicals	NBP2-32473
Human C14ORF39-C	1:30	Rabbit	This study	-
Mouse SYCP3	1:200	Mouse	Abcam	ab97672
Mouse SYCP1	1:200	Rabbit	Novus Biologicals	NB300-229
Mouse SYCE1	1:200	Rabbit	Proteintech	11063-1-AP
Mouse SIX6OS1-N	1:500	Rabbit	This study	-
Mouse SIX6OS1-C	1:500	Rabbit	This study	-
γH2AX	1:5000	Rabbit	Novus Biologicals	NB100-384
GFP	1:2000 (for WB)	Mouse	Abmart	M20004
Myc-Tag	1:1000	Mouse	Clontech	631206
Secondary antibodies				
Target	**Dilution**	**Host species**	**Supplier**	**Catalog number**
Mouse (Alexa-488)	1:100	Goat	Molecular Probes	A-21121
Rabbit (Alexa-555)	1:300	Donkey	Molecular Probes	A31572
Rat (Alexa-568)	1:150	Goat	Thermofisher	A11077
Mouse (HRP)	1:10000	Goat	Biolegend	405306
Rabbit (HRP)	1:10000	Donkey	Biolegend	406401
Rat (HRP)	1:10000	Goat	Biolegend	405405

Table S2. The sgRNAs and primers used in this study

Primers used for Sanger sequencing		
Primer name	**Sequence (5'- 3')**	**Product (bp)**
hC14orf39-MT1-Fw	TCTTAGCTTCTGGCTCTAGG	471
hC14orf39-MT1-Rv	ACATAGTGGCATAACAAGGC	
hDHRS4L2-Fw	TTAGCCACAAGACAGTTTCC	476
hDHRS4L2-Rv	CCTCAGTCTCCAGCCTATAC	
hC14orf39-MT2-Fw	CATTGGCTGGTTTCTTTGTC	682
hC14orf39-MT2-Rv	TTCCTTCAGGGATTTCTCAC	
hC14orf39-MT3-Fw	AGAAGTGGAAGATGGAACTGGA	670
hC14orf39-MT3-Rv	GCAGGAAAAATGGGGAAGAGG	
Primers used for RT-PCR		
Primer name	**Sequence (5'- 3')**	**Product (bp)**
hC14orf39-MT1-rtPCR-Fw	GCCTGTTTGTCAGTTTGGACA	455
hC14orf39-MT1-rtPCR-Rv	ACATGCCAACACTCTGCTTTG	
hC14orf39-MT2-rtPCR-Fw	TCTAGGCATAATGAAACTAAGGCTC	430
hC14orf39-MT2-rtPCR-Rv	CCCCTTTTTCCGACCACTGA	
hACTB-rtPCR-Fw	AATGAGCTGCGTGTGGCTC	148
hACTB-rtPCR-Rv	ATAGCACAGCCTGGATAGCAAC	
Primers used for qPCR		
Primer name	**Sequence (5'- 3')**	**Product (bp)**
hC14orf39-qPCR-Fw	GCCTGTTTGTCAGTTTGGACA	178
hC14orf39-qPCR-Rv	TCAATTTCCTCATCTGTTGCATT	
hACTB-qPCR-Fw	AATGAGCTGCGTGTGGCTC	148
hACTB-qPCR-Rv	ATAGCACAGCCTGGATAGCAAC	
Primers used for generation and genotyping of *Six6os1* mutant mice		
Primer name	**Sequence (5'- 3')**	**Product (bp)**
mSix6os1-exon11-sgRNA-Fw	GAAATTAATACGACTCACTATAGGGAGATCTAACAAACTTTGACTGATGTTTTAGAGC	122
mSix6os1-sgRNA-Rv	AAAAAAGCACCGACTCGGTG	
mSix6os1-exon11-Fw	ATGGTTGGAGAAATGAGGGC	476
mSix6os1-exon11-Rv	CCTGTCCTGAAACTCACACT	
mSix6os1-exon11-S-Fw	CAGATATTGTTTGGTTTTAGCTTCAG	134
mSix6os1-exon11-S-Rv	CCTGTGGATTATTTTCTTTTTGTCTC	
Primers used for plasmid construction		
Primer name	**Sequence (5'- 3')**	**Product (bp)**
AD-hC14orf39-Fw	GCCATGGAGGCCAGTGAATTCATGAATGACAGCCTGTTTGTCAG	1764
AD-hC14orf39-Rv	CAGCTCGAGCTCGATGGATCCTCAAAAAAAAGTAAACTGTGTTGTATTTTGTG	

AD-hC14orf39-Fw	GCCATGGAGGCCAGTGAATTCATGAATGACAGCCTGTTTGTCAG	215
hC14orf39 (c.204_205del)-Rv	ATCTCCTCACTGTTTACAGTAATGATCAATTTCCTCATCTG	
hC14orf39 (c.204_205del)-Fw	ACTGTAAACAGTGAGGAGATTAAAGACAACTGTAG	1571
AD-hC14orf39-Rv	CAGCTCGAGCTCGATGGATCCTCAAAAAAAAGTAAACTGTGTTGTATTTTGTG	
AD-hC14orf39-Fw	GCCATGGAGGCCAGTGAATTCATGAATGACAGCCTGTTTGTCAG	978
hC14orf39 (c.958G>T)-Rv	AAATATCTGTGTATCATTTTaTTTTTGTCTAAAGTCAATATTGGCAAGC	
hC14orf39 (c.958G>T)-Fw	TAAAATGATACACAGATATTTAATGACTCTGC	806
AD-hC14orf39-Rv	CAGCTCGAGCTCGATGGATCCTCAAAAAAAAGTAAACTGTGTTGTATTTTGTG	
BD-mSyce1-Fw	ATGGCCATGGAGGCCGAATTCATGGCCACCAGACCGCAGCC	1032
BD-mSyce1-Rv	CCGCTGCAGGTCGACGGATCCTTAGGTCCTGCTTGATGGGCGCTC	
EGFP-hC14orf39-Fw	GCATGGACGAGCTGTACAAGTCCAAGATGAATGACAGCCTGTTTGTC	1810
EGFP-hC14orf39-Rv	GATTATGATCTAGAGTCGCGTCAAAAAAAAGTAAACTGTGTTGTATTTTGTG	
EGFP-C1-hC14orf39-Fw	TCGAGCTCAAGCTTCGAATTCTATGAATGACAGCCTGTTTGTCAG	235
hC14orf39 (c.204_205del)-N-Rv	ATCTCCTCACTGTTTACAGTAATGATCAATTTCCTCATCTG	
hC14orf39 (c.204_205del)-N-Fw	ACTGTAAACAGTGAGGAGATTAAAGACAACTGTAG	1590
EGFP-C1-hC14orf39-Rv	TTATCTAGATCCGGTGGATCCTCAAAAAAAAGTAAACTGTGTTGTATTTTGTG	
EGFP-hC14orf39-Fw	GCATGGACGAGCTGTACAAGTCCAAGATGAATGACAGCCTGTTTGTC	998
hC14orf39 (c.958G>T)-N-Rv	CTGTGTATCATTTTATTTTTGTCTAAAGTCAATATTGGCAAGC	
hC14orf39 (c.958G>T)-C-Fw	GACTTTAGACAAAAATAAAATGATACACAGATATTTAATGACTCTGC	842
EGFP-hC14orf39-Rv	GATTATGATCTAGAGTCGCGTCAAAAAAAAGTAAACTGTGTTGTATTTTGTG	
mCherry-hSyce1-Fw	GCATGGACGAGCTGTACAAGggcggcggcgggtcgATGGCGGGGAGGTCCCTGAC	1111
mCherry-hSyce1-Rv	GATCTAGAGTCGCGGCCGCTTCAAAATAGCTCCTTTATTTCCTGAAAGCC	
BD-mSix6os1-Fw	GCATATGGCCATGGAGGCCGAATTCATGAATGATAATCTGTTTGTCAGTTTG	1769
BD-mSix6os1-Rv	CCGCTGCAGGTCGACGGATCCCAAAAAACATAAATTGTGTTTTATTTTGTGA	
Myc-mSix6os1-Fw	TCGAGCTCAAGCTTCGAATTCATGGAGGAGCAGAAGCTGATC	1880
Myc-mSix6os1-Rv	TTATGATCTAGAGTCGCGGCCGCAGGCCCCAAGGGGTTATGCTA	

Table S3. Overview of *C14orf39* variants identified from the affected individuals

Subjects	Genomic Position on chr14 (bp)	cDNA Change	Protein Change	Genotype	Allele Frequency in Population		
					1KGP	ESP6500	gnomAD
IV-2, IV-3 & IV-5	60483719-60483720	c.204_205del	p.His68Glnfs*2	Homozygous	0	0.0187	4.22×10^{-6}
P3097	60465993	c.958G>T	p.Glu320*	Homozygous	0	0	0
P6032	60457095	c.1180-3C>G	p.?	Homozygous	0	0	0

NCBI accession number of *C14orf39* is NM_174978.3. 1KGP, 1000 Genomes Project; gnomAD, the Genome Aggregation Database.

Supplemental References

1. Qin, Y., Jiao, X., Simpson, J.L., and Chen, Z.J. (2015). Genetics of primary ovarian insufficiency: new developments and opportunities. Hum. Reprod. Update 21, 787-808.